Separation Science and Technology
Publication details, including instructions for authors and subscription information:
http://www.informaworld.com/smpp/title~content=t713708471

Equilibrium and Fixed-Bed Adsorption of n-Hexane on Activated Carbon

W. G. Shim[a]; J. W. Lee[b]; H. Moon[a]
[a] Faculty of Applied Chemistry, Chonnam National University, Gwangju, Korea [b] Department of Chemical Engineering, Seonam University, Namwon, Korea

Online publication date: 10 September 2003

To cite this Article Shim, W. G. , Lee, J. W. and Moon, H.(2003) 'Equilibrium and Fixed-Bed Adsorption of n-Hexane on Activated Carbon', Separation Science and Technology, 38: 16, 3905 — 3926
To link to this Article: DOI: 10.1081/SS-120024711
URL: http://dx.doi.org/10.1081/SS-120024711

SEPARATION SCIENCE AND TECHNOLOGY
Vol. 38, No. 16, pp. 3905–3926, 2003

Equilibrium and Fixed-Bed Adsorption of n-Hexane on Activated Carbon

W. G. Shim,[1] J. W. Lee,[2] and H. Moon[1,*]

[1]Faculty of Applied Chemistry, Chonnam National University, Gwangju, Korea
[2]Department of Chemical Engineering, Seonam University, Namwon, Korea

ABSTRACT

Equilibrium and fixed-bed adsorption of n-hexane on pelletized activated carbon (SLG-2PS) was studied between 298.15°K and 318.15°K. Equilibrium data was obtained in a gravimetric method. Adsorption isotherms were predicted by various model equations. Based on a comprehensive comparison of various single component isotherm models, the Langmuir–Freundlich isotherm was found to provide the best fit overall for the adsorption of the adsorbates on activated carbon. Their results could also be used to simulate the adsorption and temperature experimental data. A simple mathematical model was developed to

*Correspondence: H. Moon, Faculty of Applied Chemistry, Chonnam National University, Gwangju, Korea, 500-757; Fax: + 82-62-530-1899; E-mail: hmoon@chonnam.ac.kr.

DOI: 10.1081/SS-120024711
0149-6395 (Print); 1520-5754 (Online)

www.dekker.com

MARCEL DEKKER, INC.
270 Madison Avenue, New York, New York 10016

calculate the concentration and temperature curves for the fixed bed adsorber. Model parameters were estimated from experiments and from correlations available in the literature. The mathematical model provides a good representation of the experimentally observed behavior of the breakthrough curves and temperature curves for n-hexane on activated carbon.

INTRODUCTION

Volatile organic compounds (VOC) are used as dissolving and cleaning agents in many industrial processes such as printing, film coating, and manufacturing of magnetic tapes and electronic chips. The emission of solvent vapors from these industrial processes has caused not only severe air pollution but also great loss of valuable chemicals. Therefore, the proper recovery of volatile solvent vapors from industries serves multiple purposes of reducing production cost, saving energy, and protecting the environment.

Many techniques are available for controlling VOC emissions with different advantages and limitations.[1] One of the most effective methods for controlling VOC is the adsorption process. The main advantages of adsorption, as compared with other separation techniques, are its higher selectivity and relatively higher capacity for VOC, even at low partial pressures. Activated carbon is used to remove VOC from relatively dilute concentrations in air and other gases because of its large surface area, high adsorption rate, and high mechanical strength.[2]

The primary objectives of the present work were the recovery of a solvent vapor by an adsorption process, and the theoretical analysis of adsorption bed dynamics based on a mathematical model. To obtain pertinent adsorption and desorption data and to develop a mathematical model for the calculation of a nonisothermal adsorption process, a major solvent, n-hexane, often used in many industries, was chosen, and SLG-2PS was used as adsorbents for solvent recovery.

EXPERIMENTAL STUDIES

Materials and Reagents

The adsorbent used in this study is SLG-2PS manufactured by Dong Yang Company (Korea). The arithmetic average particle diameter was determined by sieving a number of particles on a set of standard sieve trays. Various densities of carbons were measured by weighing the sample and displacing the

Marcel Dekker, Inc.
270 Madison Avenue, New York, New York 10016

Table 1. Physical properties of SLG-2PS and experimental conditions.

Property	SLG-2PS	Unit
Adsorbent		
Particle size	1.70×10^{-3}	m
Particle density	800	kg/m^3
Packing density	322.4	kg/m^3
Surface area	1221	m^2/g
Mean pore radius	25.84	Å
Column		
Temperature	308.15	K
Inner diameter	1.1×10^{-2}	m
Bed porosity	0.4	

void fraction with carbon tetra-chloride in a picnometer. Other properties, such as pore size distribution, pore volume, and specific area, were measured by N_2 adsorption in a BET system. The physical properties of the SLG-2PS are given in Table 1. Prior to use, the carbon particles were leached with boiling water for 48 hr to remove impurities from internal pores of the particles. The particles were then dried in an oven at 378.15 K. The n-hexane had 97% purity (produced by Duksan, Korea).

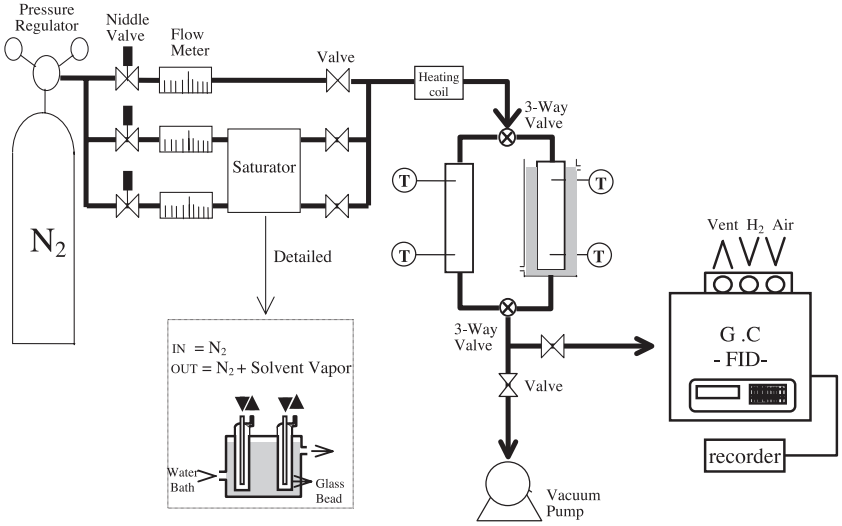

Figure 1. Schematic experimental apparatus for breakthrough experiments.

Table 2. Isotherm models.

Isotherm model	Author	Year	Model equation	Parameters
Langmuir	Langmuir	1918	$q = \frac{q_m b_1 P}{1 + b_1 P}$ $b_1 = b_{01} \exp\left(\frac{-\Delta H_A}{RT}\right)$	$q_m, b_{01}, \Delta H_A$
Modified Langmuir 1	Yang et al.	1985	$q = \frac{q_m b_1 T^{-n} P}{1 + b_1 P}$ $b_1 = b_{01} \exp\left(\frac{-\Delta H_A}{RT}\right)$	$q_m, b_{01}, \Delta H_A, n$
Modified Langmuir 2	O'Brien et al.	1984	$q = \frac{q_m b_1 P}{1 + b_1 P}\left(1 + \frac{\sigma^2(1 - b_1 P)}{2(1 + b_1 P)^2}\right)$ $b_1 = b_{01} \exp\left(\frac{-\Delta H_A}{RT}\right)$	$q_m, b_{01}, \Delta H_A, \sigma$
Langmuir–Freundlich	Sips	1948	$q = \frac{q_m b_1 P^n}{1 + b_1 P^n}$ $b_1 = b_{01} \exp\left(\frac{-\Delta H_A}{RT}\right)$	$q_m, b_{01}, \Delta H_A, n$

Toth	Toth	1971	$q = \dfrac{q_m(b_1)^{1/n}P}{(1+b_1P^n)^{1/n}}$ $b_1 = b_{01}\exp\left(\dfrac{-\Delta H_A}{RT}\right)$	q_m,b_{01},ΔH_A,n
MSL	Nitta et al.	1984	$\dfrac{q}{q_m} = n\left(1-\dfrac{q}{q_m}\right)^n \dfrac{b_1P}{T}$ $b_1 = b_{01}\exp\left(\dfrac{-\Delta H_A}{RT}\right)$	q_m,b_{01},ΔH_A,n
FH-VSM	Cochran et al.	1985	$P = \left(\dfrac{q}{b_1(1-\theta^*)}\right)\exp\left(\dfrac{\alpha_1^2\theta^*}{1+\alpha_1\theta*}\right)$ $\theta^* = \dfrac{q}{q_{mo}\exp\left(\dfrac{-h}{T}\right)}$ $b_1 = b_{01}\exp\left(-\dfrac{\Delta H_A}{RT}\right)$ $\alpha_1 = b_{02}\exp\left(-\dfrac{h}{T}\right)-1$	q_{mo},b_{01},b_{02}, ΔH_A,h

Marcel Dekker, Inc.
270 Madison Avenue, New York, New York 10016

Gravimetric Apparatus

Vapor of the solvent was generated in a small chamber that was maintained at a constant temperature. The adsorption amount of solvent vapor was measured by a quartz spring balance placed in a closed glass system. A given amount of carbon particles was placed on a dish attached to the end of the quartz spring, and the system was vacuumed for 15 hours at 10^{-3} Pa and 573.15°K to remove volatile impurities from the carbon particles. A turbomolecular pump (Edward type EXT70) in combination with a rotary vacuum pump (Edward model RV5) was used to evacuate the system. A pirani and penning vacuum gauges (Edwards Series 1000) were used for the measurement of vacuum. The pressure of the system was measured using a Baratron absolute pressure transducer (MKS instruments type 127) and a power supply read out instrument (Type PDR-C-1C). The variation of weight was measured by a digital voltmeter connected to the spring sensor. Equilibrium experiments were carried out at three different temperatures of 298.15, 308.15, and 318.15°K, respectively.

Fixed-Bed Experiments

A schematic diagram of the fixed-bed experimental setup is presented in Figure 1. The physical properties of bed characteristics are given in Table 2. The apparatus was constructed with stainless steel tubes. It consists of three major sections: 1) an apparatus for preparation of vapors, 2) an adsorption column in a water bath, and 3) an apparatus for the analysis of gas. The gas flow line of nitrogen was divided into three branches: one for pure nitrogen gas and the other two connected to solvent saturators. The concentrations of each solvent were evaluated from its saturated vapor pressure at a given temperature by assuming its vapor–liquid equilibrium state. All the lines were sufficiently heated (more than water bath) to prevent the saturated solvent vapors from condensing in the steel tubes. The gas mixture of saturated solvent vapors and pure nitrogen gas was delivered to the adsorption section. The gas flow through the column was controlled by mass flow controllers with a read-out power supply, which was precalibrated against a soap-bubble flow meter covering a wide range of flow rates under experimental pressures. The gas mixture was heated to the experimental temperature in the preheating section before being charged to the fixed-bed adsorber. Two K-type thermocouples were installed at the inlet and outlet sections of the packed column, and the temperatures were monitored continuously on a display recorder. The composition of the exit gas stream from the adsorption section was determined using a gas chromatography, GC-14B model (Shimadzu),

Marcel Dekker, Inc.
270 Madison Avenue, New York, New York 10016

equipped with a hydrogen flame ionization detector. Helium was used as a carrier gas.

THEORETICAL APPROACH

Adsorption Equilibria

In the design and optimization of adsorption separation processes, the basic experimental equilibrium data in a wide range of temperatures and concentrations is required. A number of equilibrium isotherm models have been developed over the years. The numerous isotherm models can be obtained from the Langmuir approach, the Gibbs approach, and the potential theory.[3–5] Some adsorption equilibrium models for pure component systems are shown in Table 2. The Langmuir isotherm[6] has been found to adequately describe the adsorption by substrates in many instances. However, the Langmuir isotherm is not generally useful in describing adsorption in heterogeneous systems because of its intrinsic assumption of homogeneous sorption sites. On the other hand, the Langmuir–Freundlich isotherm[7] introduced a Gaussian-like statistical function to represent the distribution of site solute interactions. This isotherm, which assumes localized adsorption without interaction among sites, has four parameters. It was presented as an expansion of the conventional Freundlich isotherm. Another useful expression is the Toth isotherm,[8] which also contains four parameters. The equation reduces to the Henry type at low concentrations and approaches the limit at high concentrations. There are also a number of other modified forms of the Langmuir isotherm. To account for the thermal expansion of the adsorbed phase, Yang and Doong[9] developed a temperature-dependent isotherm equation. Another modification model of the Langmuir isotherm, given by O'Brien and Myers,[10] proposed an expression for a single component isotherm data by a Langmuir equation with a first-order correction. In addition, this model also considered surface heterogeneity. The multisite Langmuir (MSL) model[11] is a simple, analytical, flexible as well as thermodynamically and physically consistent model. The framework for describing pure and mixed gas adsorption from adsorbates of different sizes and homogeneous and heterogeneous surface is suggested in this model. The vacancy solution theory (VSM) suggested by Suwanayuen and Danner[12] is found to be very useful for correlating single gas adsorption isotherms and gas mixture adsorption equilibria. The activity coefficients are determined by the Wilson equation. The FH-VSM model[13] was presented to correct the VSM theory. They introduced the Flory–Huggins activity coefficient to improve the VSM approach.

MARCEL DEKKER, INC.
270 Madison Avenue, New York, New York 10016

Fixed-Bed Adsorption

To study the adsorption behavior of n-hexane in a fixed-bed, a dynamic model was developed. The adsorption system considered is a nonisothermal, nonadiabatic column packed with SLG-2PS, through which an inert gas flows in steady state. This model includes the nonlinear adsorption isotherm, the mass and energy balance in the gas and solid phase, and mass transfer resistance through the adsorbent. The model adopted here utilizes the Langmuir–Freundlich isotherm equation and a linear driving force

Table 3. Mathematical model of a fixed bed.

1. Material balance

$$-D_L\frac{\partial^2 c}{\partial z^2}+\frac{\partial vc}{\partial z}+\frac{\partial c}{\partial t}+\frac{1-\varepsilon}{\varepsilon}\rho_p\frac{\partial q}{\partial t}=0$$

$$D_L\frac{\partial c}{\partial z}\bigg|_{z=0}=-v(c_{z=0^-}-c|_{z=0^+}) \quad \frac{\partial c}{\partial z}\bigg|_{z=L}=0$$

2. Heat balance, with axial thermal conduction

$$-\frac{K_z}{\varepsilon}\frac{\partial^2 T}{\partial z^2}+v\rho_g C_g\frac{\partial T}{\partial z}+\left(\rho_g C_g+\frac{1-\varepsilon}{\varepsilon}\rho_g C_s\right)\frac{\partial T}{\partial t}-$$

$$(-\Delta H_A)\frac{1-\varepsilon}{\varepsilon}\frac{\partial q}{\partial t}+\frac{2h_W}{\varepsilon R}(T-T_0)=0$$

$$K_L\frac{\partial T}{\partial z}\bigg|_{z=0}=-v\cdot\rho_g\cdot C_g\cdot(T|_{z=0^-}-T|_{z=0^+})$$

$$\frac{\partial T}{\partial_z}\bigg|_{z=L}=0$$

3. Linear driving force approximation (LDFA) model

$$\frac{\partial q}{\partial t}=k_s\cdot(q^*-q)$$

4. Adsorption isotherm: Langmuir–Freundlich

Marcel Dekker, Inc.
270 Madison Avenue, New York, New York 10016

(LDF) rate model to simplify the diffusional mass transfer inside adsorbent particles. The LDF model is a lumped-parameter model for particle adsorption. The simple mathematical model used in a fixed bed is shown in Table 3.

Determination of Model Parameters

Analyzing or designing an adsorption process requires accurate kinetic information. There are essentially three consecutive mass-transport steps associated with the adsorption of adsorbates by porous adsorbents. The mass transport through the external film of adsorbent particles is relatively fast. Therefore, the rate of adsorption in porous adsorbents is generally controlled by the intraparticle transport within the particle. For spherical particles, the external mass-transfer coefficient, k_f, can be estimated from some correlations reported in literature. Among those correlations, the equation proposed by Wakao and Funazkri[14] has been widely used for column adsorptions. The molecular diffusivity, D_m, was calculated using the Fuller equation.[15] The axial dispersion coefficient, D_L, included in the model was calculated from the correlation given by Hsu and Haynes.[16] The effective axial thermal conductivity, K_z, was estimated according to the suggestion of Yagi et al.[17] The gas density and specific heat capacity were calculated using a weighted average of the carrier and sorbate. The mass-transfer coefficient, k_s, and the wall heat transfer coefficient, h_w, were found by fitting the simulation breakthrough curves to experimental data.[18–20]

The set of coupled parabolic second-order partial differential equations cannot be solved analytically. Therefore, numerical methods have been generally employed. In this work, the complicated set of partial differential equations were first discretized by an orthogonal collocation method (OCM) to form a set of first-order ordinary differential equations (ODEs).[21,22] The resulting set of ODEs was solved using the subroutine DVODE.[23] The DVODE program employs Gear's method with variable order and step size.

RESULTS AND DISCUSSION

Adsorption Isotherm

The equilibrium isotherms of n-hexane on SLG-2PS were measured at various temperatures. The different models were used to correlate experimental equilibrium data of n-hexane on SLG-2PS. Representative

MARCEL DEKKER, INC.
270 Madison Avenue, New York, New York 10016

experimental data for n-hexane at three different temperatures, along with Langmuir–Freundlich model fits, are shown in Figure 2. The isotherm parameters for each model were determined simultaneously at all three temperatures using a pattern search algorithm namely, Nelder–Mead simplex method.[24] The comparison of fit of data by the models is based on the average relative error (ARE), which is listed in Table 4. The ARE is defined as.[25]

$$ARE = \frac{100}{N}\sum_{i=1}^{N} abs\left(\frac{Q_{cal} - Q_{\exp}}{Q_{\exp}}\right)_i \quad (1)$$

where N is the number of data points, and Q_{cal} and Q_{exp} are the calculated and experimental amounts adsorbed, respectively. In general, the Langmuir isotherm provides a less satisfactory fit compared to other isotherms. For n-hexane, the modified Langmuir isotherms 1 and 2 and the MSL isotherm does not provide any significant improvement in terms of the average relative error. On the other hand, the Langmuir–Freundlich, Toth, and FH-VSM equations all provide a very close fit of the experimental data. In

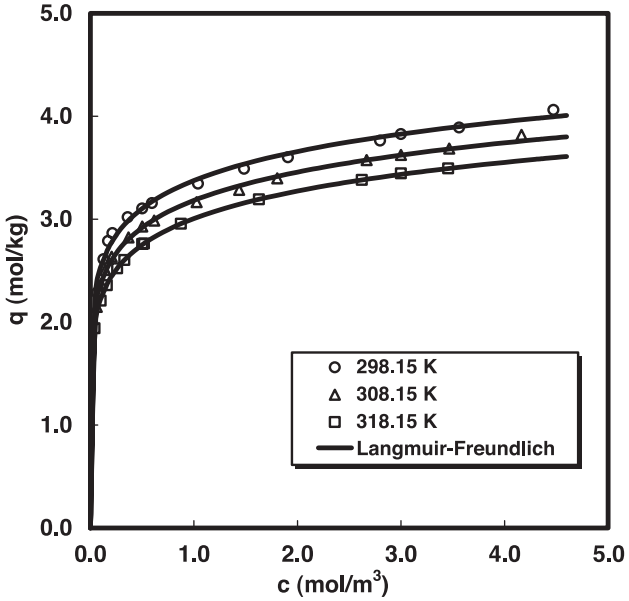

Figure 2. Adsorption equilibrium curves of n-hexane on SLG-2PS.

Table 4. Parameter values for different isotherm models.

	n-Hexane	
Isotherm model	Isotherm parameters	ARE
Langmuir	$q_m = 3.625$	6.036
	$b_{01} = 0.6139 \times 10^{-2}$	
	$-\Delta H_A = 20.017 \times 10^3$	
Langmuir–Freundlich	$q_m = 9.576$	0.828
	$b_{01} = 0.34229 \times 10^{-1}$	
	$-\Delta H_A = 68.583 \times 10^2$	
	$n = 0.1829$	
Toth	$q_m = 18.821$	0.878
	$b_{01} = 2.489$	
	$-\Delta H_A = 27.305 \times 10^2$	
	$n = 0.0729$	
Modified Langmuir 1	$q_m = 254.37$	5.984
	$b_{01} = 6.423 \times 10^{-2}$	
	$-\Delta H_A = 14.252 \times 10^3$	
	$n = 0.7440$	
Modified Langmuir 2	$q_m = 3.723$	6.912
	$b_{01} = 7.461 \times 10^{-3}$	
	$-\Delta H_A = 20.050 \times 10^3$	
	$\sigma^2 = 1.2447$	
MSL	$q_m = 3.859$	18.258
	$b_{01} = 9.940 \times 10^{-3}$	
	$-\Delta H_A = 32.587 \times 10^3$	
	$n = 1.450$	
FH-VSM	$q_{m0} = 4.143$	2.823
	$b_{01} = 5.660 \times 10^{-3}$	
	$b_{02} = 8.260 \times 10^{-3}$	
	$-h = 227.29$	
	$-\Delta H_A = 17.368 \times 10^3$	

general, the Langmuir–Freundlich isotherm shows the best results, as it provides equally good fits for n-hexane over the entire concentration range.

The characteristics of the concentration and temperature derivatives are important. These characteristics are especially important in studies on adsorption kinetics, the temperature derivative being particularly important in nonisothermal simulation.[26] Figures 3 shows $(\partial q^*/\partial C)|_T$ as a function of concentration for different types of isotherm models. The plots are for n-hexane equilibrium isotherm at a temperature of 308.15°K. Here, an important consideration is the asymptotic behavior of the isotherm at low

MARCEL DEKKER, INC.
270 Madison Avenue, New York, New York 10016

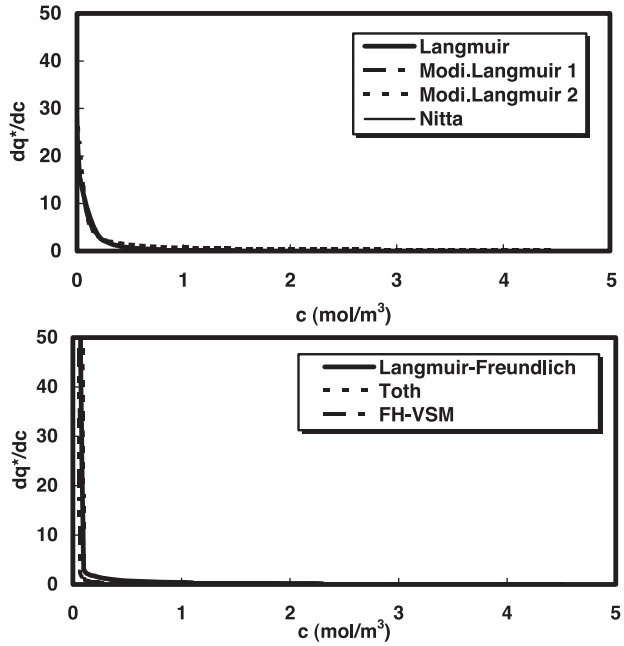

Figure 3. Concentration derivative of n-hexane equilibrium curves at 303.15°K.

coverage. From the thermodynamic definition, all adsorption isotherms should reduce to Henry's law at low coverage:

$$\lim_{P\to 0}\frac{dQ}{dP} = \lim_{P\to 0}\frac{Q}{P} = \Omega \tag{2}$$

The limiting slope, Ω, must be positive and finite gradient. In Figure 3, Langmuir, modified Langmuir 1, modified Langmuir 2, and MSL isotherm have a finite slope at low coverage. However, Langmuir–Freundlich, Toth, and FH-VSM have a large gradient at low coverage. Some isotherm equations even have thermodynamic inconsistency. These equations have been widely used so far.

The effect of the temperature derivative, $-(\partial q^*/\partial T)|_c$, for the Langmuir and Langmuir–Freundlich isotherm models with experimental data are shown in Figure 4. The temperature derivative results are very important in the nonisothermal adsorption processes. In Figure 4, Langmuir–Freundlich correlate experimental temperature derivatives at both high and low concentrations reasonably well. However, the Langmuir isotherm is not so good at the entire concentration because of the unsatisfactory equilibrium isotherm.

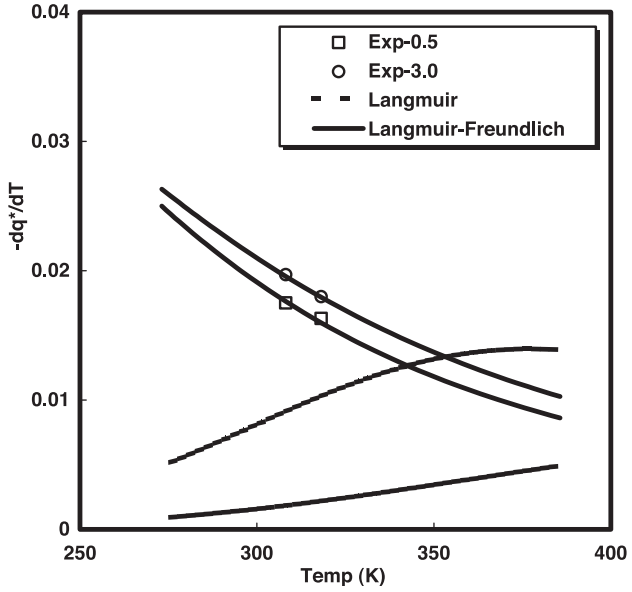

Figure 4. Temperature derivative of n-hexane equilibrium.

Fixed-Bed Adsorption

The performance of an adsorption-based process depends greatly upon the effectiveness of design and operating conditions. Therefore, rigorous approaches to the design and operation of the adsorption system must be used to ensure efficient applications. To do this, one has to understand the mechanism and dynamics of adsorption and desorption, as well as major

Table 5. Conditions of fixed-bed dynamics for the experimental conditions and model simulations.

Concentration (mol/m^3)	Length (m)	Velocity (m/s)	k_s (1/s)	h_w ($W/m^2 \cdot K$)
Adsorption				
1.5	0.090	1.78×10^{-2}	0.0020	35
2.5	0.102	1.90×10^{-2}	0.0045	34
3.6	0.082	2.20×10^{-2}	0.0075	35
Desorption				
1.5	0.090	1.81×10^{-2}	—	—
2.5	0.102	1.74×10^{-2}	—	—
3.6	0.082	1.75×10^{-2}	—	—

variables that affect the process performance. In this study, breakthrough experiments of n-hexane in SLG-2PS were performed at a various concentrations. Table 5 provides some relevant data on the adsorbents used as well as other information regarding the experiments conducted.

Before the breakthrough experiments of n-hexane through an activated carbon bed, several effects of wall heat-transfer coefficient and LDF rate coefficient were tested. The equilibrium model parameters used here were the Langmuir–Freundlich isotherm parameters for n-hexane adsorption on

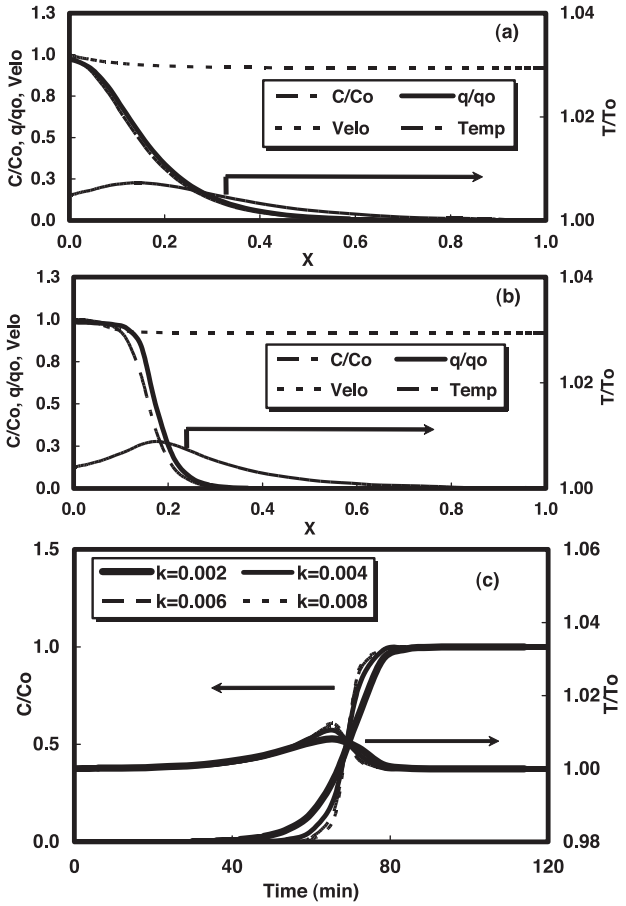

Figure 5. Effect of mass-transfer coefficient on: (a) bed profiles at 12 min ($k_s = 0.002\ s^{-1}$, $h_w = 30\ W/m^2 \cdot K$), (b) bed profiles at 12 min ($k_s = 0.008\ s^{-1}$, $h_w = 30\ W/m^2 \cdot K$), and (c) concentration and temperature breakthrough curves.

Marcel Dekker, Inc.
270 Madison Avenue, New York, New York 10016

the SLG-2PS. Using the different values of k_s and h_w, the exit concentration, temperature curves, and the bed profiles of dependent variables (*C, q, V, T*) are obtained. Figure 5 shows the effect of the mass-transfer coefficient on the concentration, temperature curves, and the bed profiles of dependent variables. As the mass-transfer coefficient increases, the exit concentration, temperature curves, and the bed profiles of dependent variables become much sharper. The mass-transfer coefficient has significant

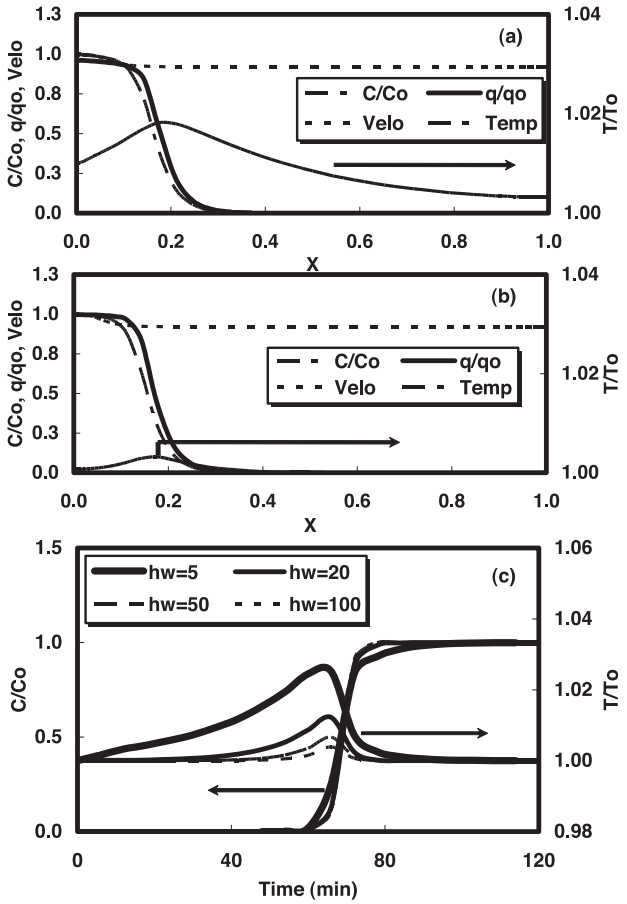

Figure 6. Effect of wall heat-transfer coefficient: (a) bed profiles at 12 min ($h_w = 5$ W/m$^2\cdot$K, $k_s = 0.008$ s^{-1}), (b) bed profiles at 12 min ($h_w = 100$ W/m$^2\cdot$K, $k_s = 0.008$ s^{-1}), and (c) concentration and temperature breakthrough curves.

MARCEL DEKKER, INC.
270 Madison Avenue, New York, New York 10016

influences on the concentration and temperature breakthrough curves. The effect of the wall-heat transfer coefficient on the concentration, temperature curves, and the bed profiles of dependent variables are shown in Figure 6. The wall heat-transfer coefficient strongly influences the temperature curves. As seen in Figure 6, the wall heat-transfer coefficient decreases with increasing temperature. One can observe that the concentration breakthrough curve is essentially unaffected by a large variation in the wall heat-transfer coefficient, while the mass-transfer coefficient strongly affected both the exit concentration and the column temperature breakthrough curves.

Figure 7 shows the effect of temperature on adsorption breakthrough curves for bed temperatures of 298.15, 348.15, 448.15, and 548.15°K. As the temperature decreases, the exit concentration breakthrough curve becomes sharper and more heat is generated during adsorption. The breakthrough curves reaching the equilibrium were slow as the temperature increases gradually. The temperature and concentration breakthrough curves appear at the end of the column at the same time (see Figure 7).

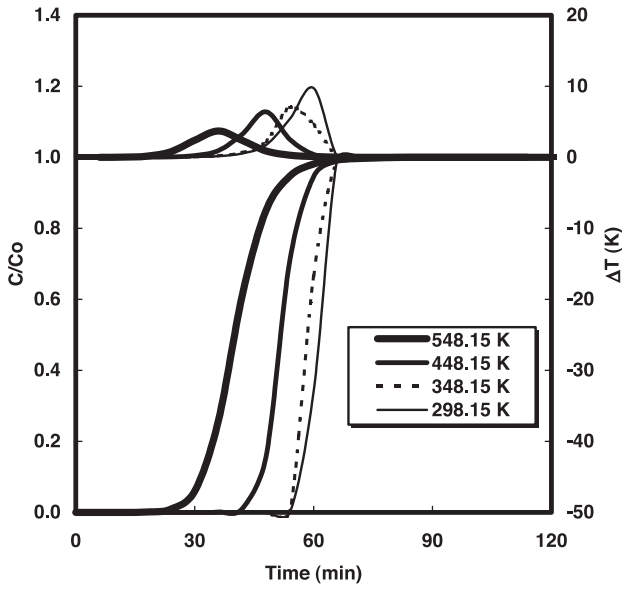

Figure 7. Effect of temperature on the concentration and temperature breakthrough curves ($c_0 = 3.0$ mol/m^3, $h_w = 30$ W/m$^2 \cdot$K).

Marcel Dekker, Inc.
270 Madison Avenue, New York, New York 10016

Figure 8 shows the effects of temperature and concentration on adsorption breakthrough curves for bed inlet concentrations of 1.5 to 3.6 mol/m^3. The temperature curve increased with the increase in inlet concentrations. Figure 8 also shows the representative fit (Langmuir–Freundlich) of theoretical concentration and temperature curves with the experimental data. The concentration and temperature breakthrough curves are increasingly sharper when the inlet concentration increases. In the case of a favorable equilibrium isotherm, the velocity of the mass-transfer zone increases and the value of slope of the adsorption isotherm decreases as the inlet concentration increases. Therefore, one could expect that higher concentration leads to higher and narrower curves, while lower concentration leads to smaller and wider curves. And the breakthrough time increased with the decrease in inlet concentrations.[3,4,18]

In actual processes, the desorption step is as important as the adsorption step since it requires a great deal of energy. The desorption breakthrough curves obtained at different experimental runs ($c_0 = 1.0 \sim 3.6$

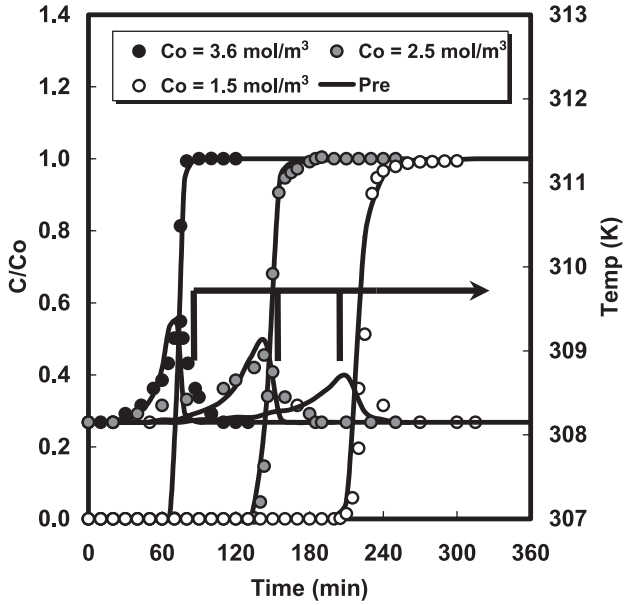

Figure 8. Adsorption and temperature breakthrough curves of n-hexane on SLG-2PS at 308.15°K ($c_0 = 3.6$ mol/m^3, $h_w = 35$ W/m$^2\cdot$K, $k_s = 0.0075$ s^{-1}; $c_0 = 2.5$ mol/m^3, $h_w = 34$ W/m$^2\cdot$K, $k_s = 0.0045$ s^{-1}; $c_0 = 1.5$ mol/m^3, $h_w = 35$ W/m$^2\cdot$K, $k_s = 0.0020$ s^{-1}).

MARCEL DEKKER, INC.
270 Madison Avenue, New York, New York 10016

mol/m^3) are shown in Figure 9. Desorption profiles are very broad and tailing because the adsorption isotherm is highly favorable. Therefore, it needs a lot of time to complete desorption. Since the desorption curves had a similar range regardless of a change in the inlet concentration of adsorption, it is possible to use the other concentration within a reasonable range when one can obtain desorption data at one concentration (see Figure 9). This means that the desorption data obtained at a concentration could be applicable to other concentrations within a reasonable range.[19]

It is essential to compare the experimental data with the result predicted from the isothermal, nonisothermal, and adiabatic models for the quantitative analysis of temperature on adsorption dynamics. Figure 10 shows the temperature breakthrough curve as it was measured at the exit of the packed column. In the case of isothermal model, it overpredicts the breakthrough time to some extent. However, the breakthrough curve predicted from the adiabatic model shows a very sharp increase in the front and then disperses in the rear zone because the adsorbates are very strongly adsorbed on activated carbon and then remain constant with high temperature. Because of a great amount of heat being stored at the rear side of the sharp adsorption front, the nonisothermal adsorption made the adsorption column play the role of a heat reservoir, reducing the adsorption

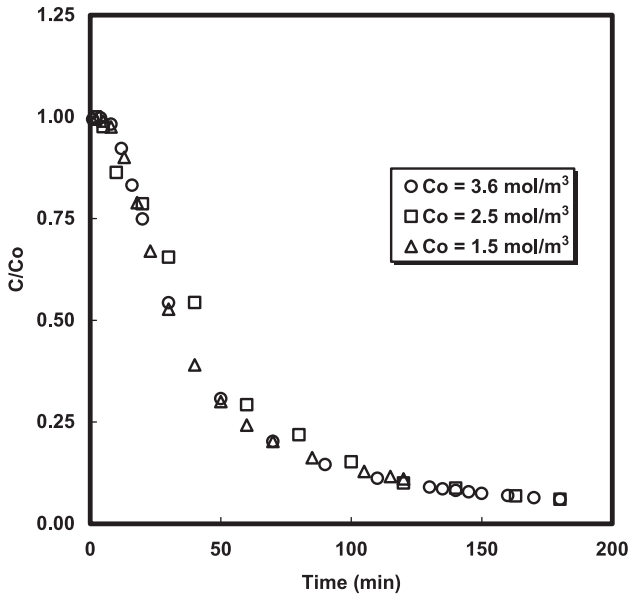

Figure 9. Desorption curves of n-hexane for various concentrations at 308.15°K.

Marcel Dekker, Inc.
270 Madison Avenue, New York, New York 10016

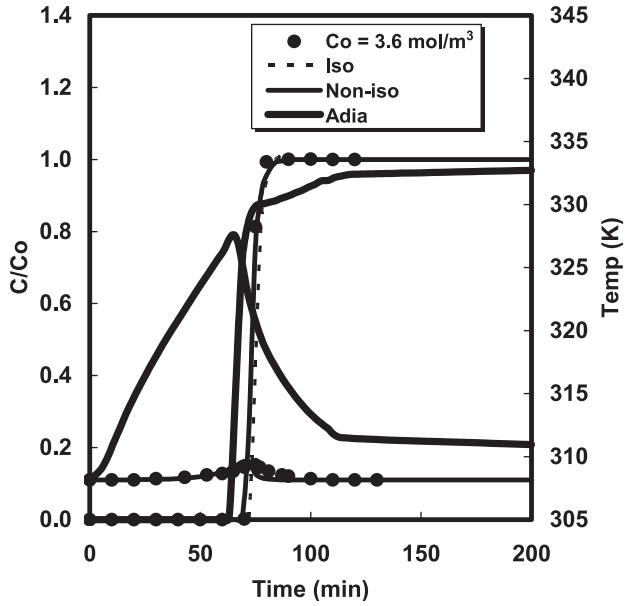

Figure 10. Typical adsorption and temperature breakthrough curves for n-hexane on SLG-2PS.

capacity of the bed.[19] In Figure 10, the isothermal model shows a prediction much closer to the nonisothermal prediction than the adiabatic one. These results testify that the isothermal operations are much more preferable in increasing the adsorption process.

CONCLUSION

Adsorption equilibrium and fixed-bed experiments were conducted to obtain pure n-hexane adsorption and regeneration data. Equilibrium data for the adsorption of n-hexane on SLG-2PS was experimentally determined at various temperatures, and the data could be fitted to the favorable-type of seven single-component isotherm models. The Langmuir isotherm is thermodynamically consistent, but it is a less satisfactory fit of the experimental data. Although the Langmuir–Freundlich isotherm is not thermodynamically consistent, it was found to be certainly superior to the others.

In the fixed-bed experiments and model predictions, the values of h_w and k_s strongly affected the concentration breakthrough curve and the

MARCEL DEKKER, INC.
270 Madison Avenue, New York, New York 10016

column temperature curve. The desorption curves were not affected by changes in feed concentration. Use of the solid-phase linear driving force mass-transfer model as a function of concentration and temperature could provide an acceptable fit to the experimental data. It can be concluded that the nonisothermal model gives the best results for the design of a real adsorption process.

ACKNOWLEDGMENT

This work was partially supported by grant No. [R-01-2001-000-00414-0 (2002)] from the Korea Science & Engineering Foundation.

NOMENCLATURE

b_1	constant in isotherm equations
b_{01},b_{02}	constant in isotherm equations
c	bulk phase concentration (mol/m^3)
c_o	sorbate concentration in the feed (mol/m^3)
C_g	gas heat capacity (J/mol·K)
C_s	particle heat capacity (J/kg·K)
D_L	axial dispersion coefficient in a fixed bed (m^2/s)
D_m	molecular diffusivity (m^2/s)
h	constant in FH-VSM equation
h_w	wall heat-transfer coefficient (W/m^2·K)
ΔH_A	heat of adsorption
k_s	LDF mass-transfer coefficient (s^{-1})
k_f	external film mass-transfer coefficient (m/s)
K_g	axial gas phase thermal conductivity (W/m·K)
K_Z	effective axial bed thermal conductivity (W/m·K)
q_m,q_{m0}	maximum adsorption capacity of adsorbent
R	gas constant (= 8.3143 *J/mol·K*)
Re	Reynolds number
R_p	particle radius (m)
Sc	Schimidt number

Greek Letters

α_1	constant in FH-VSM equation
σ	constant in FH-VSM equation
ε	bed voidage

ρ_g bulk density of adsorbent particles in a fixed bed (kg/m^3)
ρ_p particle density of adsorbent particles (kg/m^3)

REFERENCES

1. Khan, F.I.; Ghoshal, A.K. Removal of volatile organic compounds from polluted. J. Loss Prev. Proc. **2000**, *13* (6), 527–545.
2. Ruddy, E.N.; Carroll, L.A. Select the best VOC control strategy. Chem. Eng. Prog. **1993**, *89*, 28–35.
3. Ruthven, D.M. Thermodynamics of adsorption. In *Principles of Adsorption and Adsorption Processes*; Wiely: New York, 1984; 62–85.
4. Yang, R.T. Adsorbents and adsorption isotherms. In *Gas Separation by Adsorption Processes*; Butterworths: Boston, 1986; 26–48.
5. Tien, C. Representation, correlation, and prediction of single-component adsorption equilibrium data. In *Adsorption Calculations and Modeling*; Butterworths: Boston, 1994; 15–26.
6. Langmuir, I. The adsorption of gases on plane surfaces of glass, mica and platinum. J. Am. Chem. Soc. **1918**, *40*, 1361–1403.
7. Sips, R. Structure of a catalyst surface. J. Chem. Phys. **1948**, *16*, 490–495.
8. Toth, J. State equations of the solid gas interface layer. Acta Chim. Acad. Sci. Hung. **1971**, *69*, 311–317.
9. Doong, S.J.; Yang, R.T. Bulk separation of multicomponent gas mixtures by pressure swing adsorption: pore/surface diffusion and equilibrium models. AIChE J. **1986**, *32* (3), 397–410.
10. O'Brien, J.A.; Myers, A.L. Physical adsorption of gases on heterogeneous surfaces-series expansion of isotherms using central moments of the adsorption energy distribution. J. Chem. Soc., Faraday Trans. **1984**, *80* (1), 1467–1477.
11. Nitta, T.; Shigetomi, T.; Kuro-Oka, M.; Katayama, T. An adsorption isotherm of multi-site occupancy model for homogeneous surface. J. Chem. Eng. Jpn. **1984**, *17* (1), 39–45.
12. Suwanayuen, S.; Danner, R.P. A gas adsorption isotherm equation based on vacancy solution theory. AIChE J. **1980**, *26*, 68–76.
13. Cochran, T.W.; Kabel, R.L.; Danner, R.P. Vacancy solution theory of adsorption using Flory-Huggins activity coefficient equations. AIChE J. **1985**, *31* (2), 268–277.
14. Wakao, N.; Funazkri, T. Effect of fluid dispersion coefficients on particle-to-fluid mass transfer coefficients in packed beds: correlation of Sherwood numbers. Chem. Eng. Sci. **1978**, *33*, 1375–1384.
15. Fuller, E.N.; Schettler, P.D.; Giddings, J.C. A comparison of methods

MARCEL DEKKER, INC.
270 Madison Avenue, New York, New York 10016

for predicting gaseous diffusion coefficients. J. Gas Chromatogr. **1965**, *3*, 222–227.
16. Hsu, L.K.P.; Haynes, H.M. Effective diffusivity by the gas chromatography technique: analysis and application to measurement of diffusion of various hydrocarbon in Zeolite NaX. AIChE J. **1981**, *27* (1), 81–91.
17. Yagi, S.; Kunii, D.; Wakao, N. Studies on axial effective thermal conductivities in packed beds. AIChE J. **1960**, *6* (4), 543–546.
18. Silva, J.A.; Rodrigues, A.E. Fixed-bed adsorption of n-pentane/isopentane mixtures in pellets of 5A zeolite. Ind. Eng. Chem. Res. **1997**, *36*, 3769–3777.
19. Hwang, K.S.; Choi, D.K.; Gong, S.Y.; Cho, S.Y. Adsorption and thermal regeneration of methylene choloride vapor on an activatied carbon bed. Chem. Eng. Sci. **1997**, *52*, 1111–1123.
20. Malek, A.; Farooq, S. Kinetics of hydrocarbon adsorption on activated carbon and silica gel. AIChE J. **1997**, *43* (3), 761–776.
21. Finlyson, B.A. Parabolic partial differential equations time and one spatial dimension. In *Nonlinear Analysis in Chemical Engineering*; McGraw-Hill Inc.: Tokyo, 1980; 172–271.
22. Villadesen, J.V.; Stewart, W.E. Solution of boundary-value problems by orthogonal collocation. Chem. Eng. Sci. **1967**, *22*, 1483–1501.
23. Brown, P.N.; Byrne, G.D.; Hindmarsh, A.C. VODE: a variable coefficient ODE solver. SIAM J. Sci. Statist. Comput. **1989**, *10*, 1038–1051.
24. Nelder, J.A.; Mead, R. A simplex method for function minimization. Comput. J. **1965**, *7*, 308–313.
25. Kim, D.J.; Shim, W.G.; Moon, H. Adsorption equilibrium of solvent vapors on activated carbons. Korean J. Chem. Eng. **2001**, *18*, 518–524.
26. Malek, A.; Farooq, S. Comparison of isotherm models for hydrocarbon adsorption on activated carbon. AIChE J. **1996**, *42* (11), 3191–3201.

Received November 2002
Revised May 2003